RESEARCH PAPER

Generation of two-dimensional concentration-gradient droplet arrays on a two-layer chip for screening of protein crystallization conditions

Chun-Guang Yang · Yan-Hua Liu · Yue-Qin Di · Zhang-Run Xu

Abstract We developed a two-layer microfluidic chip for the generation of two-dimensional concentration-gradient droplet arrays. All of the channels, including a concentration-gradient formation channel network, an oil phase channel network, and droplet generators, were ingeniously arranged on a single polydimethylsiloxane (PDMS) substrate, which facilitates the fabrication of the chip. Ninety-six lines of subnanoliter droplets with concentration gradients can be formed on a 6-inlet PDMS chip. With the aqueous phase flow rate of 1.0 μL/min and the oil phase flow rate of 35 μL/min, relative standard deviation of the droplet sizes in the same channel was below 5.0 %, while in the 96 channels was 7.0 %. Multiparameter screening of protein crystallization conditions was demonstrated by using the two-dimensional concentration-gradient droplet arrays. Protein, precipitant, and buffer each at 16 concentrations for lysozyme crystallization were tested simultaneously in one 6-inlet chip, and five precipitants each at eight concentrations were screened at the same time in one 10-inlet chip. The concentration-gradient droplet chip proved to be a useful tool for screening crystallization conditions, characterized by low consumption, high throughput, convenience, and automatization.

Keywords Microfluidics · Concentration gradient · Droplet array · Protein crystallization · Screening

C.-G. Yang · Y.-H. Liu · Y.-Q. Di · Z.-R. Xu (✉)
Research Center for Analytical Sciences,
Northeastern University, Shenyang 110819, China
e-mail: xuzr@mail.neu.edu.cn

1 Introduction

With the advent of post-genomic era, it was discovered that the major performers of chemical reactions and cellular functions are proteins encoded by genes. Exploring the 3D crystal structures of proteins is necessary and effective for revealing their biological functions (Eisenberg et al. 2000; Ochi et al. 2009; Kim et al. 2011). Lots of methods for preparing protein crystals were developed, such as vapor diffusion, free interface diffusion, and dialysis (Chayen and Saridakis 2008). However, the preparation of high-quality protein crystals with low investment of money and labor is one of the technical bottlenecks because protein crystallization is a complex process (Saridakis and Chayen 2009; Chayen 2002; Benvenuti and Mangani 2007). Therefore, the improvement in screening throughput as well as the protein sample consumption has been widely addressed. Advances of microscale crystallization methods have been reported (Korczynska et al. 2007; D'Arcy et al. 2003, 2007; Bolanos-Garcia and Chayen 2009), in which the microbatch method is simple and efficient for high-throughput protein screening. The microbatch method significantly reduces the consumption of proteins and prevents the evaporation of the samples by dispensing and incubating a small volume of crystallization mixture under a layer of oil (Chayen 1990, 1997). Aided by robots, thousands of microbatch trials could be operated with sample consumption of nanoliter volumes (D'Arcy et al. 2004). However, the method is short of flexibility for adjusting conditions, and further increasing throughput and reducing sample consumption are hindered by the liquid dispense techniques. With the sample volume decreasing, the evaporation effect and capillary effect will have serious influences on the accuracy of dispensation.

Microfluidics featured by large scale, integration and automatization has gained widespread use in diverse fields (Reyes et al. 2002; West et al. 2008; Yang et al. 2011). Owing to good performances for handling small sample volume, controlling the mixing, and diffusion of solutions, microfluidics has the capability to perform the condition screening of protein crystallization in microchannels (Hansen et al. 2004; Guha et al. 2012; Thorson et al. 2012) as well as in microdroplets (Zheng et al. 2003, 2004). Microfluidics improved the conventional protein crystallization methods, such as vapor diffusion, free interface diffusion, dialysis, and microfluidic seeding, in terms of screening throughput, protein consumption, crystal quality, etc. (Hansen et al. 2002, 2004; Zheng et al. 2005; Li et al. 2006; Gerdts et al. 2006; Lau et al. 2007; Dhouib et al. 2009; Li et al. 2010; Li and Ismagilov 2010). Some researchers have fabricated microfluidic devices with multiple smaller microwells to replace the conventional protein crystallization microplates, which featured high throughput, good precision, and low consumption (Shim et al. 2007; Hansen et al. 2004). More benefits can be obtained from microfluidic droplet systems (Shestopalov et al. 2004; Teh et al. 2008). First, the crystallization mixtures were confined in the pL-nL level discrete droplets, and the consumption of proteins was even reduced to pL level (Hansen et al. 2004). Second, the throughput of crystallization screening was further raised owing to high droplet yield and no limitation in space (Lau et al. 2007; Hatch et al. 2011).Third, the droplets could be flexibly manipulated, and multiple condition screening was easily achieved without manual operation (Zheng et al. 2003). But there are less reports focusing on two-dimensional (2D) concentration-gradient droplet arrays for simultaneously investigating multiparameter and multicondition crystallization screening.

In our previous work, we developed a microfluidic concentration-gradient droplet array generator with parallel multichannels and multilayers (Yang et al. 2013). The generator consists of three polydimethylsiloxane (PDMS) layers. A concentration-gradient channel network and flow-focusing droplet generators were on the top layer, and an oil phase channel network was on the middle layer. The oil branch channels on the middle layer were connected, respectively, with the oil channels on the top layer via 64 access holes. The access holes were punched on the middle layer manually and were aligned with the oil channels on the top layer carefully when bonding the layers. The fabrication process is time-consuming and laborious. In this paper, we proposed a two-layer microfluidic chip for the generation of 2D concentration-gradient droplet arrays. The concentration-gradient formation channels, oil phase channels, and droplet generation channels were all arranged on a single PDMS layer. The chip is thus much easier to fabricate. The concentration-gradient droplet chip allows generating droplet arrays with precise control over droplet composition and size, which is suitable for screening multiple protein crystallization conditions. The droplets of crystallization mixtures with different components can be generated in a parallel, stable, and high-throughput pattern. Multiparameter screening was demonstrated in subnanoliter volume droplets.
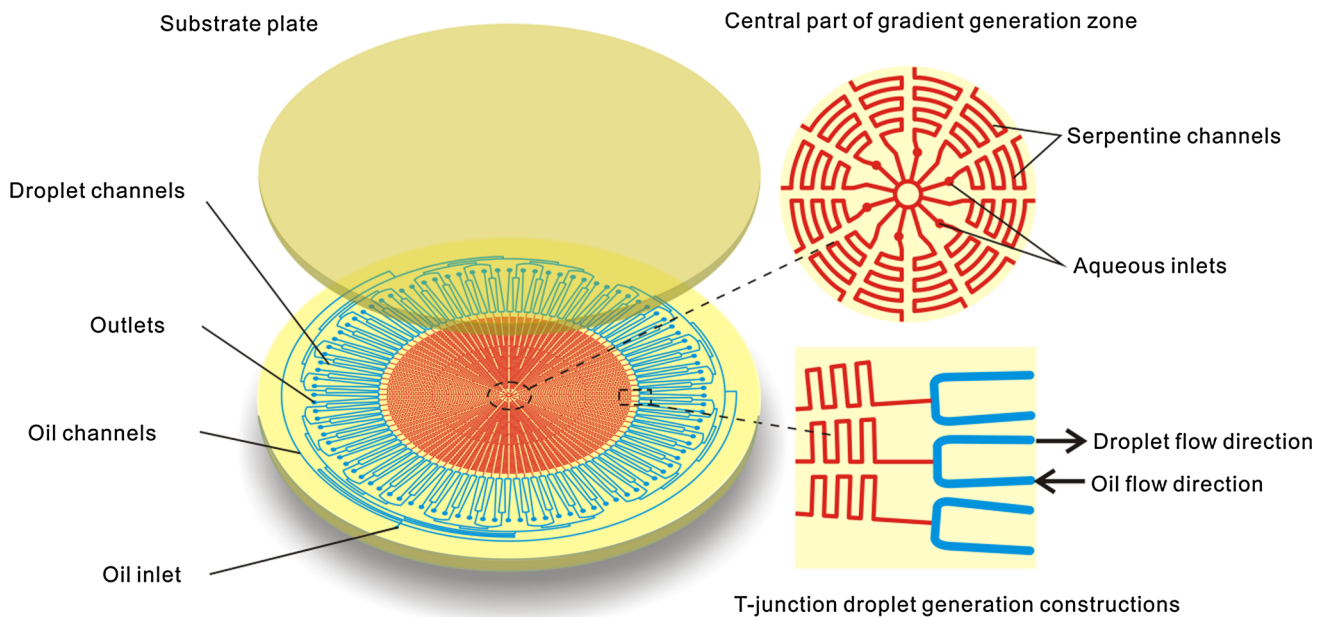
Fig. 1 Schematic diagram of the 2D concentration-gradient droplet array chip. *Left* two-layer device construct in which both concentration-gradient generation zone (*red*) and droplet generation zone (*blue*) locate on the bottom layer. *Upper right* enlarged central part of concentration-gradient generation zone. *Lower right* enlarged section of T-junction droplet generation structures (color figure online)

Table 1 Recipes of introduced solutions

Inlet	Recipes for 6-inlet chip	Recipes for 10-inlet chip
Inlet 1	50.0 mg/mL lysozyme, pH 4.74	50.0 mg/mL lysozyme, pH 4.74
Inlet 2	50.0 mg/mL lysozyme, pH 4.74 50.0 mg/mL NaCl	50.0 mg/mL lysozyme, 48.0 mg/mL K_2SO_4, pH 4.74
Inlet 3	NaCl (50.0 mg/mL), pH = 4.74	Lysozyme (50.0 mg/mL), pH = 4.74
Inlet 4	Lysozyme (50.0 mg/mL), pH = 4.74 NaCl (50.0 mg/mL)	Lysozyme (50.0 mg/mL), PEG (M = 8,000, 24.0 mg/mL), pH = 4.74
Inlet 5	Lysozyme (50.0 mg/mL), pH = 5.04 NaCl (50.0 mg/mL)	Lysozyme (50.0 mg/mL), pH = 4.74
Inlet 6	Lysozyme (50.0 mg/mL), pH = 4.44 NaCl (50.0 mg/mL)	Lysozyme (50.0 mg/mL), $MgCl_2$ (48.0 mg/mL), pH = 4.74
Inlet 7		Lysozyme (50.0 mg/mL), pH = 4.74
Inlet 8		Lysozyme (50.0 mg/mL), $MgSO_4$ (48.0 mg/mL), pH = 4.74
Inlet 9		Lysozyme (50.0 mg/mL), pH = 4.74
Inlet 10		Lysozyme (50.0 mg/mL), KCl (48.0 mg/mL), pH = 4.74

2 Materials and methods

2.1 Device design and fabrication

The device for the generation of 2D concentration-gradient droplet arrays was fabricated with PDMS (RTV615, Momentive, USA) by soft lithography techniques. Master molds of AZ P4620 (Clariant, Japan) were fabricated in clean-room facilities. One PDMS layer was replicated from the master molds and bonded with a PDMS substrate plate after air plasma treatment (Model PDC-32G, Harrick Scientific Co., USA). The layout of the two-layer PDMS chip is illustrated in Fig. 1. A concentration-gradient generator, droplet generators, and an oil phase channel network were laid out on one layer. The concentration-gradient generator is in the central part of the chip, and it is a centro-symmetric channel network including multiple circular channels and serpentine branch channels (Yang et al. 2011). The serpentine branch channels bifurcate and double in number when crossing each circular channel. The terminals of the outmost serpentine branch channels connect vertically with the oil branch channels, forming T-junctions where droplets will be generated. The aqueous inlets are located at the center of the concentration-gradient generation channel network. The oil channel network surrounds the concentration-gradient generator. The only one oil inlet locates at the outmost of the oil network. The oil phase was uniformly distributed from one inlet channel to 64 branch channels by a binary splitting network. The sections of the oil channels connecting with the aqueous phase channels are in the U-shape, and the ends of the U-shaped channels are the outlets. All of the channels are 35 µm deep. The channels of the concentration-gradient generators and the oil channels are, respectively, 56 and 112 µm wide. The diameter of the chip is 50 mm.

2.2 Formation of concentration-gradient droplets

Before use, the concentration-gradient generator was filled with aqueous phase solutions, while oil channels were filled with mineral oil. All of the fluids were introduced into the device using syringe pumps (PHD-2000, Harvard Apparatus, USA; Model MD-1001, Bioanalytical Systems, Inc., USA). Different source solutions were simultaneously introduced into the device via different aqueous phase inlets to generate the concentration gradients. The mineral oil including 2 % (v/v) Span 80 was introduced via the oil inlet. The solutions with concentration gradients in aqueous branch channels and the branch streams of oil phase met at the T-junctions. The aqueous phase solutions were dispersed into droplets and suspended in the continuous oil phases, which flowed down to the droplet outlets. The food dyes were used as aqueous phase source solutions to show the concentration gradients. Rhodamine 6G (5.0×10^{-3} g/mL) and water were chosen as aqueous phase source solutions for quantitative analysis of concentration gradients. The concentration-gradient droplets generated using the food dye solutions were recorded by a CCD (AxioCam ERc 5 s, Carl Zeiss, Germany) mounted on a stereomicroscope (Stemi 2000-C, Carl Zeiss, Germany). The fluorescence images of the concentration-gradient droplets formed using a rhodamine 6G solution of 5.0×10^{-3} g/mL (Ubichem, Hampshire, England) and water were captured by a digital gel image analysis system (Tanon-2500R, Tanon Science & Technology Co., Ltd., Shanghai, China). The fluorescence intensity of droplets was measured by the Image Pro-Plus software.

2.3 Protein crystallization on concentration-gradient droplet chips

Multiparameter screening of protein crystallization conditions was performed on the concentration-gradient droplet

chips. A 10-inlet chip was used for precipitant screening of lysozyme crystallization, and a 6-inlet chip for the multiparameter screening of a given protein-precipitant system. Quartz capillaries (ID 200 μm) were inserted into the droplet outlets as the collectors of droplets. Different solutions were simultaneously introduced into the chips via the aqueous phase inlets according to the recipes shown in Table 1. After the collection of droplets, the quartz capillaries were carefully pulled out and sealed with epoxy resin. The droplets stored in the capillaries were incubated stilly for protein crystallization. The morphology of crystal was recorded by the stereomicroscope and CCD. The protein crystal was distinguished from salt crystals by crystal violet staining (1 % crystal violet solution) and UV–Visible absorption spectrum of the crystal solution (Santhanalakshmi and Balaji 2001).

3 Results and discussion

3.1 Considerations in system design

It has been demonstrated that 2D concentration-gradient droplet arrays were able to be generated by a microfluidic concentration-gradient droplet array generator (Yang et al. 2013). However, the droplet generation structures are complicated, and the aqueous phase channels and the oil phase channels have to be arranged on two PDMS layers. The oil was introduced into a central chamber via an entry channel and distributed gradually into branch channels. For connecting the oil channels on the two layers, a series of access holes need punching and aligning carefully. As a result, the fabrication of the generator becomes a very tedious work. In this work, we designed a two-layer microfluidic chip for the generation of 2D concentration-gradient droplet arrays, which makes it much easier to manufacture complex channel structures. The oil channels were arranged surrounding the central concentration-gradient channels. The oil was introduced from an inlet, and then uniformly distributed by a binary splitting network to branch channels, which connected with the aqueous phase channels via U-shaped structures. Accordingly, the T-junction droplet generation mode was adopted for the consideration of simplifying the structures. Thus, the concentration-gradient channel network and the oil phase channel network were integrated into one layer. The newly designed chip was fabricated without having to punch any oil phase access holes and align the access holes. The fabrication process is more time-saving and easier. In addition, more aqueous phase inlets were designed to introduce more aqueous source solutions into the device at the same time, which benefits the generation of multiple concentration gradients for multiparametric

screening. The number of the aqueous phase branch channels depends on the number of inlets and the times of splitting. The number of downstream channels is doubled after the upstream channels split in the present work. With the number of the inlets M and the times of splitting N, the number of branch channels, i.e., the number of outlets, is ($M{\cdot}2^N$). Each aqueous phase branch channel corresponds to one oil droplet channel. The set number of concentration-gradient droplet arrays depends on the number of inlets. The ($M{\cdot}2^N$) droplet channels consist of M sets of concentration-gradient droplet arrays, and there are 2^N droplet channels in each set. We have fabricated two types of concentration-gradient droplet chips in this work,
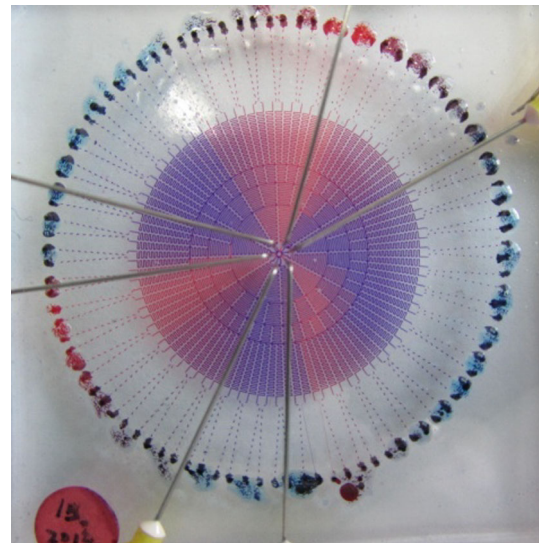
Fig. 2 Images of 6-inlet chip filled with two food dye solutions each of which was injected from three alternate inlets
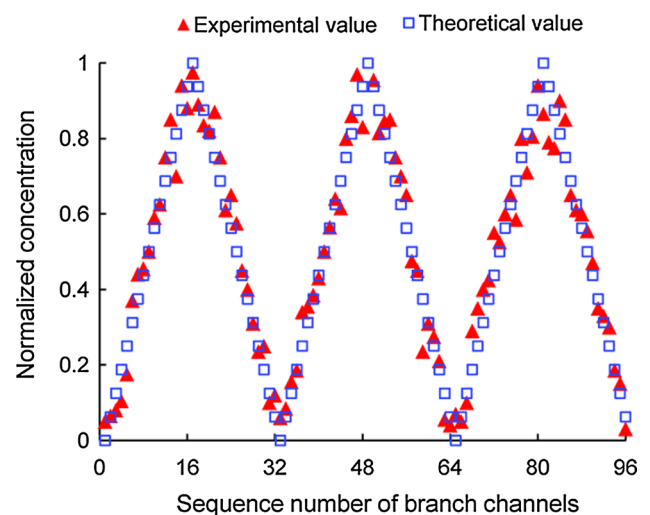

Fig. 3 Concentration-gradient curves generated in the 6-inlet chip (*hollow square*, theoretical value; *triangle*, experimental value)

which, respectively, possess six aqueous phase inlets and ten aqueous phase inlets. In the 6-inlet chip, the aqueous phase solutions entered 96 branch channels after being split and combined four times, and met, respectively, with the oil in 96 U-shaped channels forming 96 droplet generation units, as shown in Fig. 1. The oil imposed hydrodynamic force on the concentration-gradient solutions from branch channels at the T-junctions, and the solutions were dispersed into droplets. The droplets had the same concentration gradient with the aqueous solutions upstream. Thus, 96 droplet arrays can be generated in the 6-inlet chip, and they include six sets of concentration-gradient droplet array, as shown in Fig. 2. The concentration-gradient droplet arrays can be formed in 5 min, and it can last for at least 4 h. The 2D concentration-gradient droplet arrays can be generated simultaneously in all the branch channels. The chip is qualified for the parameter screening for multiple chemical objects, and the concentration gradients of the droplets can be produced in a parallel and high-throughput pattern. And this design can handle more chemical source solutions by increasing the number of aqueous phase inlets, which is further verified by operating the 10-inlet chip in this work.

3.2 Characterization of the device

In the 6-inlet chip, 96 solutions were formed at the terminals of the 96 aqueous branch channels after four times of splitting and mixing process. And then, the 96 lines of droplets were generated at the T-junction structures due to the perpendicular shear force of oil phases (Thorsen et al. 2001) and flowed along one arm of each U-shaped oil channel to the outlets. In our previous work, two sets of concentration-gradient droplet arrays formed in a 2-inlet chip (Yang et al. 2013). In each set, the concentration gradient ranged within the two boundary concentrations, which were the concentrations of the two aqueous source solutions. In the present work, six sets of concentration-gradient droplet arrays were generated in the 6-inlet chip. To measure the concentration distribution of droplet arrays, rhodamine 6G solution and deionized water were alternately introduced via the 6 inlets to form concentration-gradient droplets of rhodamine 6G. When exposed under the excitation light, the droplets can emit fluorescence. The concentrations of rhodamine 6G in the droplets can be calculated according to the fluorescence intensities. To make it easier for discussion, the concentration value of
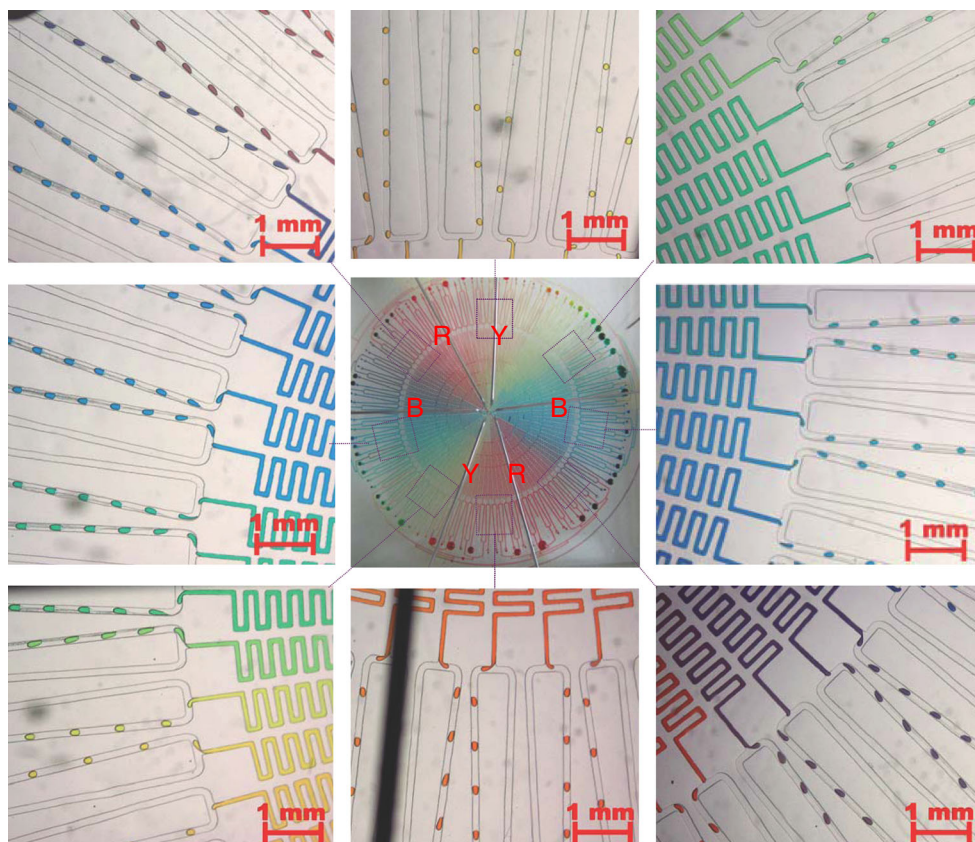

Fig. 4 Images of the concentration-gradient droplet array formed by introducing three food dye source solutions. The colors of source solutions at 6 inlets are *yellow* (Y), *blue* (B), *red* (R), *yellow* (Y), *blue* (B), and *red* (R) in order (color figure online)

rhodamine 6G source solution is regarded as 1 and the water as 0. Figure 3 shows the concentration-gradient curves generated in the 6-inlet chip. The boundary channels, channel 0, 32, and 64 (channel 0 and channel 96 are the same channel), were filled with water, while the other boundary channels, channel 16, 48, and 80, were filled with rhodamine 6G source solutions. Thus, six concentration-gradient zones were formed. In each concentration-gradient zone, the concentrations of droplets decrease by 1/16 step by step from the boundary channels of rhodamine 6G source solution to the adjacent boundary channels of water in theory. The regression equations of the six sets are, respectively, $y = 0.0627x + 0.0013$ $(0 \leq x \leq 16,\ r^2 = 0.9639)$, $y = -0.0599x + 1.9618$ $(16 \leq x \leq 32,\ r^2 = 0.9756)$, $y = 0.0599x - 1.8773$ $(32 \leq x \leq 48,\ r^2 = 0.9744)$, $y = -0.0649x + 4.1479$ $(48 \leq x \leq 64,\ r^2 = 0.9666)$, $y = 0.0534x - 3.3300$ $(64 \leq x \leq 80,\ r^2 = 0.9497)$, and $y = -0.0563x + 5.4530$ $(80 \leq x \leq 96,\ r^2 = 0.9510)$, where y stands for normalized concentration and x for sequence number of branch channel. The theoretical concentration gradients were adequately verified by the experimental concentrations of droplets, although the disparity between the theoretical values and the experimental values was observed. One reason causing the disparity is that the slight flaws in the channels and heterogeneous property of the channel surface might cause inconsistency of the splitting ratios. The other reason is that the uneven exciting light of the imaging equipment might bring about the experimental error. Actually, the concentrations at each branch channels can be predicted easily according to the branch channel number and the level number (Yang et al. 2011). In the present work, the normalized concentration of dye source solution is defined as 1, the boundary channel injected with source solutions is defined as the 0th channel, and the adjacent channels are orderly defined as the first, second, third, … …, 16th channel. Thus, the theoretical value at the xth $(0 \leq x \leq 16)$ channel is $(1 - x/16)$. To further show the gradient profiles, three food dye solutions were alternately fed into the 6-inlet chip. Figure 4 shows 2D concentration-gradient droplet arrays generated using yellow, purple, and red dyes. The 96 lines of droplets similarly divided into six sets according to the channel location. The colors of droplets in each set gradually change from one dye to the other. It should be noted that the size and shape of the droplets with different colors are not uniform. The reason is that the dye solutions with different components have different surface tensions, which influence the formation of the droplets.

The droplet generation results from the combined effect of several forces: interfacial tension, viscous force, hydraulic pressure, etc. (Teh et al. 2008; Yang et al. 2010). The formation of droplets in a T-junction is quite subtle. It consists of three distinct regimes: squeezing, dripping, and jetting (de Menech et al. 2008). The droplet generation frequency and droplet volume are affected by interfacial tension, the channel aspect ratio, flow rate ratio, and viscosity ratio (Wehking et al. 2014). In the present work, we simply changed the interfacial tension by adding surfactant Span 80 (2 % v/v) into the oil phase for stabilizing the droplets. The effects of the flow rate and the flow rate ratio of the two phases on the droplet size were investigated. A low aqueous phase flow rate of 1.0 μL/min at each inlet was chosen to obtain small-size droplets. The different oil phase flow rates at the inlet ranging from 5 to 35 μL/min were investigated with the constant aqueous phase flow rate of 1.0 μL/min, and their effects on the droplet size were shown in Fig. 5. The results of the experiment indicate that the length of the droplets decreases and the monodispersity of the droplets improves with the increase in the flow rates of oil phases. The shortest length of
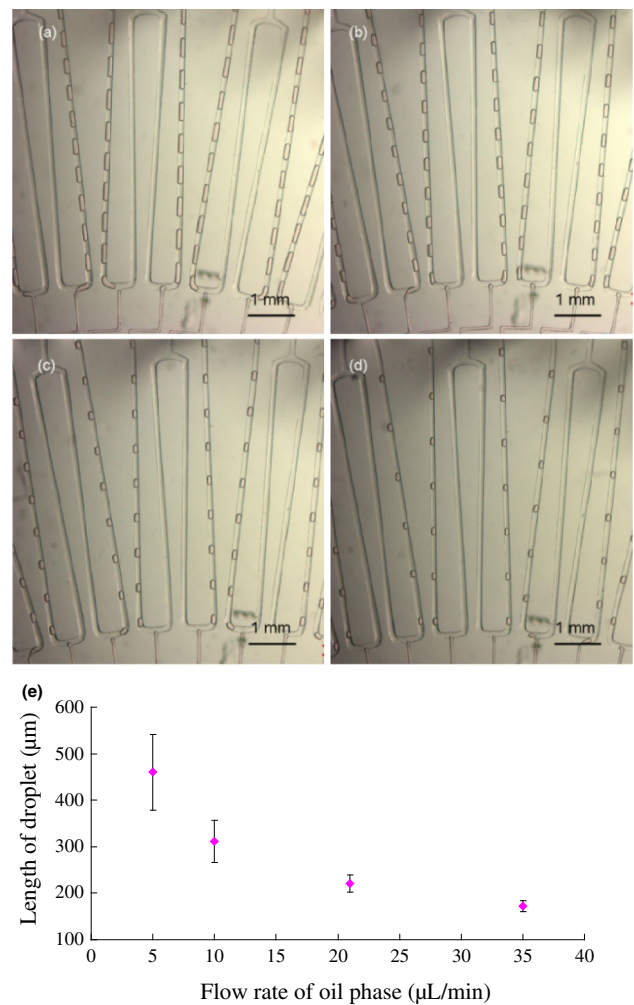
Fig. 5 **a–d** Images of the droplets generated with the aqueous phase flow rate of 1 μL/min and the oil phase flow rates of 5 μL/min (**a**), 10 μL/min (**b**), 21 μL/min (**c**), and 35 μL/min (**d**). **e** Effect of the oil phase flow rates on droplet length with the aqueous phase flow rate of 1.0 μL/min

170 μm (about 0.57 nL) and best monodispersity were obtained under the aqueous phase flow rate of 1.0 μL/min and the oil phase flow rate of 35 μL/min. Relative standard deviation of the droplet length was below 5.0 % in the same channel and 7.0 % in the 96 channels.

3.3 Protein crystallization screening

The concentration-gradient droplet chip can be fed with various solutions that were diluted, respectively, to a series of solutions with quantitative concentrations and then the diluted solutions formed 2D droplet arrays. The characterization of the chip exactly corresponds with the needs of protein crystallization condition screening. In this work, using the 6-inlet concentration-gradient droplet chip, 48 different crystallization conditions were screened simultaneously in one 6-inlet chip. Lysozyme was used as the model protein, sodium chloride as the precipitating agent, and acetic acid–sodium acetate as the pH buffer. The mixtures were simultaneously introduced into the channel network according to the recipes in Table 1. Ninety-six lines of droplets were generated, and their theoretical contents in the droplets of each line were illustrated in the Fig. 6a. The 17 concentration gradients of precipitant NaCl ranging from 0 to 50 mg/mL are shown in channel 0–16 with invariable conditions of 50 mg/mL lysozyme and pH

4.74. The precipitant concentration difference between the droplets in adjacent channels is 3.1 mg/mL. A symmetrical gradient profile of lysozyme with 17 theoretical concentrations ranging from 0 to 50 mg/mL in droplet channel 16–48 will be formed with constant conditions of 50 mg/mL NaCl and pH 4.74. The pH gradients are shown in channel 48–64 with a difference of 0.02 and in the other 17-line droplets in channel 64–80 with a difference of 0.04. In channel 80–96, the double variable parameters of precipitant and pH value will be formed, with the NaCl concentration decreasing at 3.1 mg/mL and pH value increasing at 0.02 from channel 80 to 96. Therefore, the effects of lysozyme concentration, precipitant concentration, and pH value on protein crystallization can be investigated at the same time on a single chip. In addition, the screening of precipitant type can also be performed using the concentration-gradient droplet chip with 10 aqueous phase inlets. Five precipitants, K_2SO_4, $MgCl_2$, $MgSO_4$, KCl, and PEG, were introduced to the 10-inlet chip according to the recipes shown in Table 1. The theoretical concentration ranges of precipitants are shown in Fig. 6b. The concentrations of K_2SO_4, $MgCl_2$, $MgSO_4$, and KCl all range from 6 to 48 mg/mL, and the concentrations of PEG vary from 3 to 24 mg/mL. Each precipitant of eight concentrations was investigated, and each concentration was formed in two lines except the maximum concentration.

Fig. 6 Theoretical values of chemicals in droplets. **a** 6-inlet chip; **b** 10-inlet chip
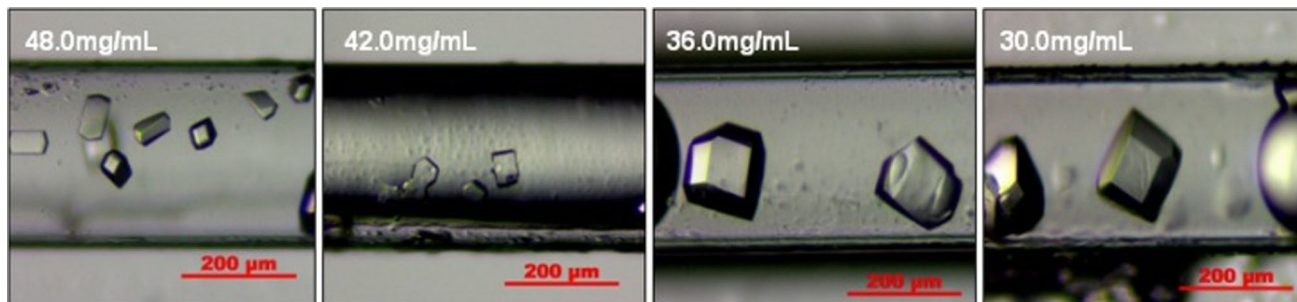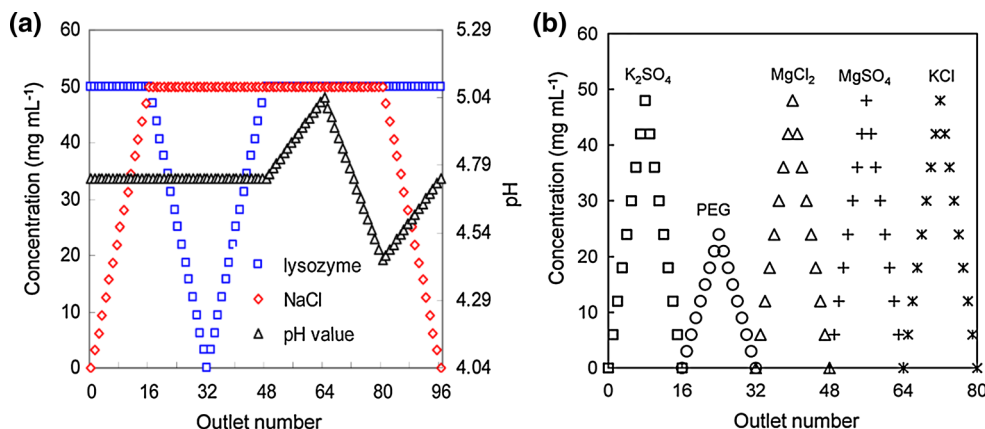
Fig. 7 Photographs of the lysozyme crystals obtained by, respectively, using $MgCl_2$ solutions of 48.0, 42.0, 36.0, and 30.0 mg/mL as the precipitants

After the collection, the droplets were incubated in capillaries for the lysozyme crystals growing. Crystallization of proteins inside droplets was monitored and recorded under microscope and camera. In all the droplets of 16 lysozyme concentrations, crystals were observed. The crystals appeared after 2 h in the droplets with the lysozyme concentrations higher than 30 mg/mL, while appeared after 12 h in the droplets with the lysozyme concentrations below 30 mg/mL. The crystal shape was better when the lysozyme concentrations were within the range of 30–45 mg/mL. The crystals were observed after 2 h in all of the droplets containing precipitant NaCl ranging from 3.1 to 50 mg/mL. When NaCl concentrations were higher than 35 mg/mL, many fine crystals were generated. The desired crystals were formed when NaCl concentrations were between 20 and 30 mg/mL. The crystals in the droplets exhibited regular prism shape when the pH values ranged within 4.8–4.9. When the pH value was below 4.8, the shape of the crystals became irregular and even rod-like crystals appeared. For screening of five types of precipitants, high-quality lysozyme crystals were obtained only when using $MgCl_2$ as the precipitant, as shown in Fig. 7. It demonstrates that $MgCl_2$ is a candidate precipitant for lysozyme crystallization.

4 Conclusions

We presented a microfluidic concentration-gradient droplet chip with a simple structure of two-layer PDMS and multi-inlet for the generation of 2D concentration-gradient droplet arrays. A concentration-gradient generator and multiple T-junction droplet generators were integrated to form dozens of concentration-gradient droplet arrays with subnanoliter volume and good monodispersity at the same time. Multiparameter screening of protein crystallization was achieved using the concentration-gradient droplet chip. The effects of protein, precipitant, and buffer on the crystal quality were evaluated simultaneously in one single chip. Five precipitants with 8 concentrations for each were screened at the same time by a 10-inlet chip. The device can be used as a versatile platform for microfluidic protein crystallization, which avoids the redundant procedure of preparing sample and precipitant solutions with various concentrations.

References

Benvenuti M, Mangani S (2007) Crystallization of soluble proteins in vapor diffusion for x-ray crystallography. Nat Protoc 2(7):1633–1651

Bolanos-Garcia VM, Chayen NE (2009) New directions in conventional methods of protein crystallization. Prog Biophys Mol Biol 101(1–3):3–12

Chayen NE (1990) An automated system for micro-batch protein crystallization and screening. J Appl Crystallogr 23(4):297–302

Chayen NE (1997) The role of oil in macromolecular crystallization. Structure 5(10):1269–1274

Chayen NE (2002) Tackling the bottleneck of protein crystallization in the post-genomic era. Trends Biotechnol 20(3):98

Chayen NE, Saridakis E (2008) Protein crystallization: from purified protein to diffraction-quality crystal. Nat Methods 5(2):147–153

D'Arcy A, Mac Sweeney A, Stihle M, Haber A (2003) The advantages of using a modified microbatch method for rapid screening of protein crystallization conditions. Acta Crystallogr D 59:396–399

D'Arcy A, MacSweeney A, Haber A (2004) Practical aspects of using the microbatch method in screening conditions for protein crystallization. Methods 34(3):323–328

D'Arcy A, Villard F, Marsh M (2007) An automated microseed matrix-screening method for protein crystallization. Acta Crystallogr D 63:550–554

De Menech M, Garstecki P, Jousse F, Stone HA (2008) Transition from squeezing to dripping in a microfluidic T-shaped junction. J Fluid Mech 595:141–161

Dhouib K, Malek CK, Pfleging W, Gauthier-Manuel B, Duffait R, Thuillier G, Ferrigno R, Jacquamet L, Ohana J, Ferrer JL, Theobald-Dietrich A, Giege R, Lorber B, Sauter C (2009) Microfluidic chips for the crystallization of biomacromolecules by counter-diffusion and on-chip crystal X-ray analysis. Lab Chip 9(10):1412–1421

Eisenberg D, Marcotte EM, Xenarios I, Yeates TO (2000) Protein function in the post-genomic era. Nature 405(6788):823–826

Gerdts CJ, Tereshko V, Yadav MK, Dementieva I, Collart F, Joachimiak A, Stevens RC, Kuhn P, Kossiakoff A, Ismagilov RF (2006) Time-controlled microfluidic seeding in nL-volume droplets to separate nucleation and growth stages of protein crystallization. Angew Chem Int Ed 45(48):8156–8160

Guha S, Perry SL, Pawate AS, Kenis PJA (2012) Fabrication of X-ray compatible microfluidic platforms for protein crystallization. Sens Actuators B 174:1–9

Hansen CL, Skordalakes E, Berger JM, Quake SR (2002) A robust and scalable microfluidic metering method that allows protein crystal growth by free interface diffusion. Proc Natl Acad Sci USA 99(26):16531–16536

Hansen CL, Sommer MOA, Quake SR (2004) Systematic investigation of protein phase behavior with a microfluidic formulator. Proc Natl Acad Sci USA 101(40):14431–14436

Hatch AC, Fisher JS, Pentoney SL, Yang DL, Lee AP (2011) Tunable 3D droplet self-assembly for ultra-high-density digital microreactor arrays. Lab Chip 11(15):2509–2517

Kim Y, Babnigg G, Jedrzejczak R, Eschenfeldt WH, Li H, Maltseva N, Hatzos-Skintges C, Gu M, Makowska-Grzyska M, Wu R, An H, Chhor G, Joachimiak A (2011) High-throughput protein purification and quality assessment for crystallization. Methods 55(1):12–28

Korczynska J, Hu TC, Smith DK, Jenkins J, Lewis R, Edwards T, Brzozowski AM (2007) Microscale vapour diffusion for protein crystallization. Acta Crystallogr D 63:1009–1015

Lau BTC, Baitz CA, Dong XP, Hansen CL (2007) A complete microfluidic screening platform for rational protein crystallization. J Am Chem Soc 129(3):454–455

Li L, Ismagilov RF (2010) Protein crystallization using microfluidic technologies based on valves, droplets, and SlipChip. Annu Rev Biophys 39:139–158

Li L, Mustafi D, Fu Q, Tereshko V, Chen DL, Tice JD, Ismagilov RF (2006) Nanoliter microfluidic hybrid method for simultaneous screening and optimization validated with crystallization of membrane proteins. Proc Natl Acad Sci USA 103(51):19243–19248

Li G, Chen Q, Li J, Hu X, Zhao J (2010) A compact disk-like centrifugal microfluidic system for high-throughput nanoliter-scale protein crystallization screening. Anal Chem 82(11):4362–4369

Ochi T, Bolanos-Garcia VM, Stojanoff V, Moreno A (2009) Perspectives on protein crystallisation. Prog Biophys Mol Bio 101(1–3):56–63

Reyes DR, Iossifidis D, Auroux PA, Manz A (2002) Micro total analysis systems. 1. Introduction, theory, and technology. Anal Chem 74(12):2623–2636

Santhanalakshmi J, Balaji S (2001) Binding studies of crystal violet on proteins. Colloid Surf A 186(3):173–177

Saridakis E, Chayen NE (2009) Towards a 'universal' nucleant for protein crystallization. Trends Biotechnol 27(2):99–106

Shestopalov I, Tice JD, Ismagilov RF (2004) Multi-step synthesis of nanoparticles performed on millisecond time scale in a microfluidic droplet-based system. Lab Chip 4(4):316–321

Shim JU, Cristobal G, Link DR, Thorsen T, Fraden S (2007) Using microfluidics to decouple nucleation and growth of protein crystals. Cryst Growth Des 7(11):2192–2194

Teh SY, Lin R, Hung LH, Lee AP (2008) Droplet microfluidics. Lab Chip 8(2):198–220

Thorsen T, Roberts RW, Arnold FH, Quake SR (2001) Dynamic pattern formation in a vesicle-generating microfluidic device. Phys Rev Lett 86(18):4163–4166

Thorson MR, Goyal S, Gong YC, Zhang GGZ, Kenis PJA (2012) Microfluidic approach to polymorph screening through antisolvent crystallization. Crystengcomm 14(7):2404–2412

Wehking JD, Gabany M, Chew L, Kumar R (2014) Effects of viscosity, interfacial tension, and flow geometry on droplet formation in a microfluidic T-junction. Microfluid Nanofluid 16:441–453

West J, Becker M, Tombrink S, Manz A (2008) Micro total analysis systems: latest achievements. Anal Chem 80(12):4403–4419

Yang CG, Xu ZR, Wang JH (2010) Manipulation of droplets in microfluidic systems. TrAC Trends Anal Chem 29(2):141–157

Yang CG, Wu YF, Xu ZR, Wang JH (2011) A radial microfluidic concentration gradient generator with high-density channels for cell apoptosis assay. Lab Chip 11(19):3305–3312

Yang CG, Xu ZR, Lee AP, Wang JH (2013) A microfluidic concentration-gradient droplet array generator for the production of multi-color nanoparticles. Lab Chip 13(14):2815–2820

Zheng B, Roach LS, Ismagilov RF (2003) Screening of protein crystallization conditions on a microfluidic chip using nanoliter-size droplets. J Am Chem Soc 125(37):11170–11171

Zheng B, Tice JD, Roach LS, Ismagilov RF (2004) A droplet-based, composite PDMS/glass capillary microfluidic system for evaluating protein crystallization conditions by microbatch and vapor-diffusion methods with on-chip X-ray diffraction. Angew Chem Int Ed 43(19):2508–2511

Zheng B, Gerdts CJ, Ismagilov RF (2005) Using nanoliter plugs in microfluidics to facilitate and understand protein crystallization. Curr Opin Struct Biol 15(5):548–555